



Published in final edited form as:

J Immunol. 2008 January 1; 180(1): 238–248.

The Inhibitory HVEM-BTLA Pathway Counter Regulates Lymphotoxin β Receptor Signaling to Achieve Homeostasis of Dendritic Cells ¹

Carl De Trez ^{*}, Kirsten Schneider ^{*}, Karen Potter ^{*}, Nathalie Droin ^{*}, James Fulton ^{*}, Paula S. Norris ^{*}, Suk-won Ha ^{*}, Yang-Xin Fu [†], Theresa Murphy [‡], Kenneth M. Murphy [‡], Klaus Pfeffer [§], Chris A. Benedict ^{*}, and Carl F. Ware ^{*,2}

^{*}Division of Molecular Immunology, La Jolla Institute for Allergy and Immunology, La Jolla, CA 92037

[†]Department of Pathology, University of Chicago, Chicago, IL 60637

[‡]Department of Pathology and Immunology, Howard Hughes Medical Institute, Washington University School of Medicine, St. Louis, MO 63110

[§]Institute of Medical Microbiology, University of Düsseldorf, Düsseldorf, Germany

Abstract

Proliferation of dendritic cells (DC) in the spleen is regulated by positive growth signals through the lymphotoxin (LT)- β receptor; however, the countering inhibitory signals that achieve homeostatic control are unresolved. Mice deficient in LT α , LT β , LT β R, and the NF κ B inducing kinase show a specific loss of CD8⁺ DC subsets. In contrast, the CD8 α ⁺ DC subsets were overpopulated in mice deficient in the herpesvirus entry mediator (HVEM) or B and T lymphocyte attenuator (BTLA). HVEM- and BTLA-deficient DC subsets displayed a specific growth advantage in repopulating the spleen in competitive replacement bone marrow chimeric mice. Expression of HVEM and BTLA were required in DC and in the surrounding microenvironment, although DC expression of LT β R was necessary to maintain homeostasis. Moreover, enforced activation of the LT β R with an agonist Ab drove expansion of CD8 α ⁺ DC subsets, overriding regulation by the HVEM-BTLA pathway. These results indicate the HVEM-BTLA pathway provides an inhibitory checkpoint for DC homeostasis in lymphoid tissue. Together, the LT β R and HVEM-BTLA pathways form an integrated signaling network regulating DC homeostasis.

Dendritic cells (DC)³ are bone marrow-derived APCs that play a crucial role bridging innate and adaptive immune responses through the activation of naive Ag-specific T cells (1). Expression of CD11c, in addition to the common hemopoietic markers CD11b, F4/80, CD24 (HSA), CD205 (DEC-205), aid in defining DC subpopulations in mouse lymphoid organs (2). Three main subpopulations of CD11c^{high} expressing DC are present in the mouse spleen,

¹This work supported in part by grants from the Public Health Service, National Institutes of Health, AI33068, CA69381, AI48073, and AI06789.

Copyright © 2007 by The American Association of Immunologists, Inc.

²Address correspondence and reprint requests to Dr. Carl F. Ware, Division of Molecular Immunology, La Jolla Institute for Allergy and Immunology, 9420 Athena Circle, La Jolla, CA 92037. E-mail address: E-mail: cware@liai.org.

Disclosures

The authors have no financial conflict of interest.

³Abbreviations used in this paper: BTLA, B and T lymphocyte attenuator; HVEM, herpesvirus entry mediator; ICSBP, IFN consensus sequence binding factor; IRF, IFN response factor; LIGHT, LT-related inducible ligand that competes for glycoprotein D binding to HVEM on T cells; LT, lymphotoxin; NIK, NF κ B-inducing kinase; pDC plasmacytoid DC; wt, wild type.

the CD8 α^+ DC subset, and the CD4 $^+$ and a CD8 α^- CD4 $^-$ dual negative subsets, the latter two forming the CD8 α^- DC subset. The CD4 $^+$ and CD8 α^- DC subsets are principally localized in the marginal zone bridging channels, and extend in the red pulp whereas the CD8 α^+ DC are found in the T cell-rich area in the white pulp (3). Several lines of evidence indicate that DC subsets possess distinct functions, although both CD8 α^+ and CD8 α^- DC present Ag to T cells (4,5). A fourth subset of splenic DC is the plasmacytoid DC (pDC), which expresses low levels of CD11c (B220 $^+$ CD11b $^-$) and are distinguished functionally by secretion high levels of type I IFNs in response to challenge with viral and bacterial pathogens (6,7). In the lymph node, two additional DC subsets can be delineated by relatively low expression of CD8, high levels of MHC II with either moderate or high expression of DEC-205 (8).

The pathways regulating the development and homeostasis of DC subpopulations are unresolved (9). Cellular reconstitution studies showed that CD8 α^+ thymic and splenic DC are derived from early CD4 $^{\text{low}}$ thymic precursors, leading to the idea that some DC could have a lymphoid origin (10,11). However, such a pathway seems less likely in view of the observations that common myeloid progenitor cells as well as lymphoid progenitors can differentiate into both CD8 α^- and CD8 α^+ DC subsets (12–14). More recent evidence indicates that a resident DC precursor gives rise to conventional CD8 $^-$ and CD8 α subsets independently of pDC (15). Genetic analysis of DC development and homeostasis has revealed distinct genes control the major DC subsets. The CD8 α^+ DC subset is affected by genetic deficiency in ICSBP (IFN consensus sequence binding factor), also called IRF-8 (IFN response factor-8), Id2 (helix-loop-helix family transcription factor inhibitor DNA binding-2), and Jak3 (Janus tyrosine kinase) (16–18). By contrast, genes involved in the differentiation of the CD8 α^- DC subset include Ikaros C $^{-/-}$, transcription factor PU.1, IRF-2 and IRF-4 (IFN regulatory factor), Notch-dependent transcription factor RBP-J, TRAF6 (TNF receptor associated factor-6), and RelB (NF κ B) and lymphotoxin- β receptor (LT β R) (19–26).

Recent evidence indicates the LT β R is a growth regulator of DC in lymphoid tissues (26). TNF does not appear to play this role but does influence DC differentiation in the bone marrow; however, LT $\alpha^{-/-}$, LT $\beta^{-/-}$ and LT β R $^{-/-}$ mice exhibit normal bone marrow DC subsets (27). In contrast, dysregulation of DC in peripheral lymphoid organs is apparent in LT-deficient mice, but was previously thought to be a result of disrupted architecture and loss of chemokines. Recent evidence lessens that possibility and supports the idea that LT β R provides a key signal for self-renewal directly to CD8 α^- DC subsets (26). Interestingly, RelB is a downstream target of LT β R signaling (28) raising the possibility these molecules function in a common pathway regulating growth of CD8 α^- DC subsets.

Counter regulatory pathways should exist that operate to limit the growth promoting actions of the LT β R pathway in DC. However, the LT β R is one constituent of a multicomponent system of interconnected signaling pathways, with no defined inhibitory systems that would directly counter regulate signaling. The LT β R binds two ligands, the membrane LT $\alpha\beta$ complex and LIGHT (LT-related inducible ligand that competes for glycoprotein D binding to herpesvirus entry mediator on T cells), yet LIGHT also engages the herpesvirus entry mediator (HVEM) (TNFRSF14) (29,30). The LIGHT-HVEM pathway appears to play a prominent role as a positive cosignaling pathway during T cell activation akin to its TNFR paralogs (e.g., 4-1BB, O x 40, CD27) (31). Adding to the complexity is the recent observation that HVEM engages a non-canonical ligand, B and T lymphocyte attenuator (BTLA) (32). BTLA, a member of the Ig superfamily, is activated by HVEM binding, attenuating Ag receptor signals through an ITIM/ITSM-dependent recruitment of Src homology phosphatase-1 or -2 (33,34). BTLA and LIGHT bind HVEM at distinct sites (35–37), yet membrane-anchored LIGHT can noncompetitively displace BTLA, suggesting HVEM serves as a molecular switch between positive and inhibitory signaling (35). HVEM-BTLA pathway plays an inhibitory role in regulating T cell proliferation (38–41). The interconnectedness of these cytokines is further

underscored by the binding of secreted $LT\alpha$ to both receptors for TNF, in addition to HVEM (29). The multicomponent nature of the $LT\alpha\beta$ /LIGHT systems precludes a clear assignment of the pathways involved in regulating DC homeostasis, which is further complicated by the multiple cell types including Ag-activated T and B lymphocytes, NK cells and lymphoid tissue inducer (LTi) cells expressing the various ligands and receptors.

In this study, using mice genetically deficient in the various components of the $LT\alpha\beta$ /LIGHT pathways and pharmacological modulation of the $LT\beta R$ pathway, we demonstrate that $LT\alpha\beta$ - $LT\beta R$ via $NF\kappa B$ -inducing kinase (NIK) is the predominant signaling pathway that positively regulates the growth of $CD4^+$ and $CD8\alpha^{-/4^-}$ DC subsets in lymphoid tissues. By contrast, HVEM- and BTLA-deficient mice both show a specific increase in the $CD4^+$ and $CD4^-$ $CD8\alpha$ DC subsets, providing a counteracting, inhibitory checkpoint in the accumulation of DC in lymphoid tissues. Together the results indicate homeostasis of DC within lymphoid tissues is achieved by integration of positive and inhibitory signals through the $LT\alpha\beta$ - $LT\beta R$ and HVEM-BTLA pathways.

Materials and Methods

Mice and reagents

C57BL/6 (B6) and $LT\alpha^{-/-}$ were purchased from The Jackson Laboratory. Mice deficient in $LT\beta R^{-/-}$ (42), $LIGHT^{-/-}$ (43), $LT\beta^{-/-}$ (44), $LT\beta/LIGHT^{-/-}$ (43), $HVEM^{-/-}$ (45), *alymploplasia* (*aly*) (46), or $BTLA^{-/-}$ (47) were inbred in the C57BL/6 background. $LT\beta/LIGHT/HVEM^{-/-}$ mice were generated by backcrossing the indicated strains and bred at the LIAI. All the knockout mice used in this study were backcrossed for: $LT\beta$, $n = 10$ generations; $LT\alpha$, $n = 8$ and the others $n = 5$. Sex- and age-matched male and female mice between 7 and 10 wk of age were used in all experiments. Mice were treated with the mouse $LT\beta R$ -Fc decoy receptor or agonistic anti- $LT\beta R$ Ab (4H8) by i.p. injection of 100 μg of each reagent every 3 to 4 days. These reagents were prepared as described (48). All breeding and experimental protocols were performed under the approval by LIAI Animal Care Committee.

Cell preparation from lymphoid organs Flow cytometry

Spleens were perfused with balanced salt solution containing collagenase (0.35 mg/ml; CLSIII; Worthington Biochemical), incubated for 30 min at 37°C in HBSS medium containing collagenase (1.4 mg/ml) and further dissociated in 2 mM EDTA saline and passage through a 70 μm nylon mesh filter. Spleen cells were analyzed by flow cytometry with a FACS-Calibur cytofluorometer (BD Bioscience) with FlowJo software (Tree Star). The cells were blocked with anti-FcR 2.4G2 (anti-Fc receptor; BD Pharmingen) and then stained with fluorescein (FITC)-coupled anti-CD11c- (N418), or PE-coupled anti- $CD8\alpha$ (53-6.7), anti-Ly6G (1A8), anti-PDCA-1 (Miltenyi Biotec), PerCp-coupled anti-B220, anti-CD11b (M1/70) or allophycocyanin-coupled anti-CD4 (L3T4), anti-CD11b (M1/70) or anti-F4/80 (BM8) (BD Pharmingen). HVEM and BTLA were detected on cells previously blocked with anti-FcR 2.4G2 by incubation with a rat anti-mouse HVEM (14C1.1) and hamster anti-C57BL/6 BTLA (6A6). Anti-rat IgM-PE or anti-Armenian hamster IgG-PE (BD Pharmingen) were used as the chromophores, respectively. In parallel, rat IgM or hamster IgG Abs were used as controls for nonspecific background staining. The background staining was similar to staining obtained with the specific anti-HVEM or anti-BTLA-specific Abs of cells from HVEM- or BTLA-deficient mice, respectively (data not shown). Cells were gated according to size and scatter to eliminate dead cells and debris from analysis.

BrdU labeling

Mice were administered BrdU (2 mg/mouse) i.p. for a 16 h pulse. Splenocytes were stained with anti-CD4-PE, anti-CD8 α -PerCp and anti-CD11c-allophycocyanin. BrdU incorporation was visualized using FITC BrdU detection kit (BD Pharmingen) and flow cytometry.

Bone marrow chimeras

Bone marrow chimeric mice were generated by i.v. transfer of bone marrow cells (5×10^6) from LT β R-deficient or C57BL/6 mice into previously lethally irradiated (9.5 Gy, Cesium) C57BL/6 and LT β R-deficient recipients. Bone marrow was isolated from donor femurs and tibias and depleted of RBC. Eight weeks after reconstitution, flow cytometry was used to analyze DC subsets.

Quantitative PCR

Eight weeks after reconstitution, spleens from LT β R chimera were recovered, snap frozen in liquid nitrogen and total mRNA from spleen was isolated with Trizol (Invitrogen), digested with DNase and reverse transcribed. cDNA was used for real-time PCR on a MX4000 with SyBr Green detection protocol as outlined by the manufacturer. Sequence-specific chemokine primers are available from the corresponding author.

Results

LT α β -LT β R signaling regulates DC homeostasis

The LT β R utilizes at least two distinct ligands, the heterotrimeric LT α 1 β 2 complex and LIGHT, both of which activate the LT β R. To distinguish the roles of these two ligands in DC homeostasis, C57BL/6 (B6) mice deficient in LT β (LT β ^{-/-}), LT α (LT α ^{-/-}), or LIGHT (LIGHT^{-/-}) were analyzed by flow cytometry for the major DC subsets in the spleen in comparison to wild-type (wt) and LT β R^{-/-} mice. The total number of CD11c^{high} cells from the spleen was reduced in LT β ^{-/-} and LT α ^{-/-} mice when compared with wt B6 mice in a pattern identical to LT β R^{-/-} mice (Fig. 1A). The ratio of CD8 α to CD4⁺ DC subsets in wt B6 mice is 0.5; however, this ratio was inverted in LT β (2.0), LT α (2.0), and LT β R-deficient mice (1.7). The inverted DC ratio in the LT-deficient mice reflected a specific decrease in the percentage (Fig. 1B) and total numbers of CD4⁺ and CD8 α ⁻/4⁻ DC subsets (Fig. 1C).

LT β R signaling controls the expression of several chemokines required for the maturation of the splenic architecture, which might effect migration of DC in the adult animal. However, the specific loss of these DC subsets in LT β R^{-/-} mice was independent of the expression of lymphoid organizing chemokines, CCL21 (SLC), CCL19 (ELC), and CXCL13 (BLC) as determined with bone marrow chimeras that isolated LT β R expression in either the bone marrow or the radioresistant stroma (Fig. 2). LT β R^{-/-} recipients reconstituted with wt B6 bone marrow had normal CD4⁺ and CD8 α ⁻/4⁻ DC subsets, yet chemokine levels were as depressed as LT β R^{-/-} mice, whereas in the reciprocal chimeras (LT β R^{-/-}→B6) chemokine expression was normal, but the DC subset ratio was inverted. These results indicate the DC phenotype in LT-deficient mice was not due to impaired maturation of the splenic architecture.

In contrast to LT-deficient mice, genetic deficiency in LIGHT, a second ligand for LT β R, showed normal cellularity in DC and a normal CD8 α /CD4 DC ratio ($r = 0.5$) (Fig. 1). Mice deficient in both LT β and LIGHT (LT β /LIGHT^{-/-}) revealed an inverted CD8 α /CD4 DC ratio ($r = 2.2$) suggesting no additional role of LIGHT in controlling the number of DC in the spleen (Fig. 1). However, we observed a difference in the size of the spleen from LT β and LIGHT/LT β -deficient mice. An accounting of the cellularity revealed increased number of cells in the spleen of LT β , LT α , and LT β R-deficient mice relative to wt mice (cellularity increased 45, 56, and 67%, respectively), proportionally effecting all the major lymphoid and myeloid

subpopulations, with a corresponding enlargement of the spleen (Fig. 3). Deleting *LIGHT* in the $LT\beta^{-/-}$ mice decreased the total number of cells in the spleen to that of wt mice. Although the total number of cells decreased, which gives the appearance of an additional effect on DC subsets, the ratio of $CD8\alpha/CD4$ (2.2) remained inverted in the $LT\beta/LIGHT^{-/-}$ suggesting that *LIGHT* was not influencing $CD8\alpha$ DC subset. Previous work attributed the increase in the total number of splenocytes in *LT*-deficient mice to the lack of peripheral lymphoid organs (42), however, that notion is inconsistent with the observation that lymph nodes and Peyer's Patches are also missing in the $LT\beta/LIGHT^{-/-}$ mice (43). This result also lessens the likelihood that the migration of immediate DC precursor population to the spleen was affected in the $LT\beta/LIGHT^{-/-}$ mice (49). That the effect of *LIGHT* on splenic size and cellularity occurred only in the absence of $LT\beta$ suggests that *LIGHT* counter regulates the $LT\alpha\beta$ - $LT\beta R$ pathway to influence cellularity of the spleen.

The HVEM-BTLA pathway provides an inhibitory checkpoint for the homeostasis of $CD8\alpha^{-}$ DC subsets

The finding that DC subsets were normal in the $LIGHT^{-/-}$ mice raised the issue of whether HVEM-BTLA pathway was involved in regulating DC homeostasis. Surprisingly in contrast to mice deficient in $LT\beta R$ signaling, $HVEM^{-/-}$ mice had a significantly higher percentage of DC in the spleen with an altered $CD8\alpha/CD4$ DC ratio (0.3) reflecting a specific increase in the $CD4^{+}$ and $CD8\alpha^{-}/4^{-}$ DC subsets compared with wt mice (Fig. 4A). *BTLA*-deficient mice displayed an identical phenotype to the $HVEM^{-/-}$ mice, with reduced $CD8\alpha/CD4$ DC ratio (0.3) resulting also from an increase in $CD4^{+}$ and $CD8\alpha^{-}/4^{-}$ DC subsets when compared with wt mice (Fig. 4B).

All of the conventional DC subsets in spleens of B6 mice express HVEM, *BTLA* (Fig. 4C), and $LT\beta R$ (26). Interestingly, *BTLA* expression was detectable on $CD4^{+}$ and $CD8\alpha^{-}/4^{-}$ subsets but more prominent on $CD8\alpha^{+}$ DC subset (Fig. 4C). Thus, all DC express the potential to deliver and receive information via the HVEM-BTLA pathway.

DC homeostasis depends on intrinsic expression of the $LT\beta R$ (26) (Fig. 2) raising the issue of whether HVEM and *BTLA* expression is required in the hemopoietic or stromal compartments. To test this issue, we generated mixed bone marrow chimeric mice. The results demonstrate that DC from $BTLA^{-/-}$ bone marrow (CD45.2) were much more abundant (6.2-fold) than the DC from wt (CD45.1) in wt recipients, although the $CD45.2/CD45.1$ ratio of total spleen cells was approximately 1 in reconstituted mice indicating equivalent potential of cells from wt or deficient mice to replenish the spleen (Table I). $HVEM^{-/-}$ DC (CD45.2) also showed an enhanced capacity (4.6-fold) to reconstitute the spleen of wt recipient mice. Reconstitution of the DC pool in recipients deficient in HVEM or *BTLA* expression moderated the advantage of DC lacking *BTLA* (wt/*BTLA*→*BTLA*; CD45 ratio = 2.0) or HVEM (wt/*HVEM*→*HVEM*; CD45 ratio = 2.8) compared with wt recipients suggesting the radioresistant stroma contributes to HVEM-BTLA dependent regulation of DC.

Analysis of the DC subsets in the mixed chimeras presented a more complex picture on the role of HVEM-BTLA in regulating splenic DC (Table I). The ratio of $CD8\alpha/CD4$ DC subsets in the $CD45.2^{+}$ population in the wt or $BTLA^{-/-}$ recipients were nearly equivalent ($r \approx -0.3$) and identical to the ratio in *BTLA* null mice. In contrast, the wt/*HVEM* mixed chimeras displayed a ratio = 0.6, near wt, that was due to an increase in the $CD45.2^{+}$ $CD8\alpha$ DC subset. This result suggested that HVEM intrinsically regulates $CD8\alpha$ DC subset. Interestingly, the $CD45.1$ DC displayed a $CD8\alpha/CD4$ ratio = 0.3, independent of recipient background, indicating that the absence of HVEM in the $CD45.2$ DC population can affect the $CD8\alpha^{-}$ subsets in wt DC.

To address whether the inhibitory function of HVEM-BTLA pathway was dominant relative to LT β R signaling, we generated mice deficient in all three “ligands” by crossing LT β /LIGHT $^{-/-}$ mice with HVEM $^{-/-}$ mice. The percentage and numbers of DC in spleens from the triple deficient mice were similar to the LT β /LIGHT $^{-/-}$ mice (Fig. 5), but the ratio of CD8 α /CD4 DC subsets was comparable to wt (0.6), reflecting a decrease in the CD8 α^+ subset and an increase in the CD4 $^+$ subset (Fig. 5). Although the LT β /LIGHT $^{-/-}$ mice displayed decreased CD8 α^+ DC cell numbers because of the relative smaller spleen and cell numbers already discussed, the inclusion of HVEM deficiency further decreased the number of cells in the CD8 α^+ DC subset, yet the CD4 $^+$ subset increased (Fig. 3B) restoring the ratio to that of wt (0.6). This observation was confirmed in BTLA $^{-/-}$ mice treated with the LT β R-Fc decoy, which neutralizes both LIGHT and LT $\alpha\beta$. LT β R-Fc decoy treated BTLA $^{-/-}$ mice exhibited decreased DC cellularity and the subset ratio was altered to $r=0.6$, recapitulating the phenotype of the triple deficient mice (Fig. 6). The ability of LT β R-Fc decoy treatment to modulate DC supports the idea that continuous LT β R signaling is required for the homeostasis of CD8 α^- DC subsets, diminishing the likelihood this phenotype is due to a genetic artifact or a developmentally fixed defect.

Other hemopoietic cells including pDC, granulocytes, monocytes and macrophages in the spleen were unaffected in the triple deficient mice or in the LT β R-Fc decoy treated BTLA $^{-/-}$ mice (data not shown). Deletion of HVEM in the triple-deficient mice did not alter the size of the spleen or the total number of splenocytes that was observed in the LT β /LIGHT $^{-/-}$ mice, indicating the HVEM-BTLA pathway does not contribute to this phenotype.

The LT $\alpha\beta$ -LT β R and HVEM-BTLA pathways regulate different phases of DC homeostasis

Although the previous results indicated that both LT $\alpha\beta$ -LT β R and HVEM-BTLA pathways regulated the same DC subsets, it was not clear whether these pathways converge at a common or distinct phase in DC differentiation. We took a pharmacological approach to address whether enforced activation of the LT β R with an agonist mAb would act in dominant or recessive fashion to HVEM-BTLA. Administration of the anti-LT β R mAb over a 14-day period increased the percentage of splenic DC in LT β /LIGHT $^{-/-}$ mice with a specific rise in the CD8 α^- subsets to levels that the CD8 α /CD4 DC ratio (0.3) exceeded the ratio in wt mice (Fig. 7, A and B), and comparable to mice lacking either HVEM or BTLA (Fig. 4, A and B). A modest effect was observed in the CD8 α^+ DC subset. Similar results were also obtained in LT α -deficient mice after administration of the agonistic anti-LT β R Ab, however treatment of LT β R $^{-/-}$ mice with the agonist anti-LT β R had no effect on the DC compartment confirming the specificity of this Ab (data not shown). Surprisingly, when the agonist LT β R Ab was administered to wt mice the cellularity of DC in the spleen also increased, as did the percentage of CD8 α^- DC subsets, with the total number of cells exceeding that of wt (Fig. 7C). The effect of the agonist anti-LT β R was reflected in the increase in the percentage of DC, but not in a major shift in the CD8 α /CD4 DC ratio, which is in contrast to the response in LT β /LIGHT $^{-/-}$ mice. Thus, the effect of the agonist anti-LT β R appeared to override the inhibitory action of HVEM-BTLA, suggesting LT β R signaling is dominant or functions independently of HVEM-BTLA.

The proliferation inducing activity of LT β R signaling in the CD8 α^- DC subsets can be measured by nucleotide (bromideoxyuridine, BrdU) incorporation in dividing DC (26). The division of both mature DC and their immediate precursors are represented in the population during the 16 h BrdU labeling period. The number of cells specifically incorporating BrdU increased in the CD4 $^+$ and CD8 α^- DC subsets in HVEM $^{-/-}$ and BTLA $^{-/-}$ mice reflecting a net accumulation of cells in those subsets (Fig. 7D). As expected, dramatically fewer cells incorporated BrdU in LT β /LIGHT-deficient mice, which is consistent with the corresponding loss in the percentage of proliferating cells in each DC subset (Fig. 7D, bottom panel). However,

there was no significant change in the percentage of proliferating cells within each subset in either HVEM^{-/-} or BTLA^{-/-} mice when compared with wt mice. This result indicates that the inhibitory effect of HVEM-BTLA does not impinge on the LTβR-dependent proliferation of DC.

We addressed whether the LTβR and HVEM-BTLA pathways could be distinguished at the level of down stream signaling pathways by examining the noncanonical NFκB pathway. LTβR signaling activates the formation of Rel B/p52 complex by inducing the processing of p100, the precursor form of p52, which is dependent on NIK. HVEM also has the potential to activate the NIK-dependent RelB NFκB pathway (50). Mice harboring a defective NIK gene (alymphoplasia, *aly*) (46) exhibited a DC profile identical to mice deficient in LTα, LTβ, or LTβR with decreased percentage of CD11c^{high} DC and an inverted CD8α/CD4⁺ DC ratio (2.0), specifically reflecting the decreased cellularity of CD4⁺ and CD8α-4- DC subsets (Fig. 8). Moreover, NIK mutant mice had a larger spleen with increased cellularity, a phenocopy of mice deficient in LTβR, LTα or LTβ (Fig. 3). However, pDC, granulocytes, monocytes and macrophages in *aly* mice were similar to normal B6 mice (data not shown). The similarity in phenotype of *aly* mice suggests that NIK acts in a common pathway with LTαβ-LTβR to regulate DC homeostasis. The results further suggest that BTLA is not activating HVEM to engage NIK in regulating DC homeostasis.

Discussion

The identification of the HVEM-BTLA system as an inhibitory checkpoint for the LTαβ-LTβR pathway defines a novel mechanism regulating the homeostatic equilibrium of resident DC populations in lymphoid tissues. The HVEM-BTLA inhibitory pathway primarily impacts the CD8α- DC subsets in the spleen, the same populations that expand in response to LTαβ-LTβR signaling. A majority (~70%) of the resident DC in the adult mouse spleen are under dynamic control by the LTαβ-LTβR and HVEM-BTLA pathways. However, a basal level of DC, with a normal ratio of CD8α to CD4 subsets, was maintained in the spleen in the absence of LTαβ, LIGHT and HVEM indicating a second distinct mechanism operates to control DC populations in the spleen. It is not known if these cells are proliferating. Inhibitory signaling requires expression of HVEM and BTLA in DC and cells in the stromal microenvironment. Together, the LTαβ-LTβR and HVEM-BTLA pathways provide key signals that integrate to achieve homeostasis of DC in lymphoid tissues.

Positive signaling provided through the LTβR controls the proliferation and differentiation of the CD8α- DC subsets or their precursors within peripheral lymphoid tissues (26). Intrinsic expression of the LTβR in hemopoietic compartment was necessary for DC proliferation, and as shown here, LTαβ is the key ligand mediating DC proliferation under homeostatic conditions. The positive signals provided by LTαβ-LTβR pathway specifically increased the number of cells in the CD4⁺ and CD8α-4- DC subsets (Fig. 1). Moreover, an identical phenotype was observed in mice with mutant NIK (*aly*) (Fig. 8) or *relB* (25) implicating the involvement of the NFκB2 processing pathway initiated by LTαβ-LTβR mediates positive signals for DC homeostasis. Restoration of the CD4⁺ and CD8α-4- DC subsets in LTβ/LIGHT deficient mice with an agonist anti-LTβR mAb demonstrated that LTβR signaling is sufficient for promoting proliferation and differentiation of the LT-regulated DC subsets. Moreover, the effect of the LTβR-Fc decoy on specific DC subsets demonstrated the dynamic aspect of LTβR signaling required for maintaining DC in the spleen. This result also indicated that the DC defect in LT-deficient mice is not a developmental “fixed” phenotype, as is, for example, the formation of lymph nodes (51). LTβR signaling regulates lymphocyte recirculation across high endothelial venules (52), which could also impact immigration of DC precursors into the spleen (49). The increased splenic cellularity in LT deficient mice probably reflects this alteration of recirculation (Fig. 3), yet the phenotype was corrected in the LTβ/LIGHT double

deficient mice, which renders altered immigration to a minor role as a mechanism accounting for LT β R's function in regulating DC populations.

Mice deficient in either HVEM or BTLA revealed an inhibitory pathway for DC that primarily affected the CD4⁺ and CD8 α -/4- DC subsets, the same subsets dependent on LT β R pathway (Fig. 4). The competitive advantage of HVEM or BTLA deficient DC in repopulating the spleen, a phenotype expected for cells alleviated from an inhibitory pathway, clearly demonstrated the impact of this pathway in restricting DC proliferation and accumulation (Table I). The similarity in this DC phenotype supports the substantial biochemical data that HVEM and BTLA form a signaling pathway (32,35,37). Interestingly, the genotype of the stromal cells in the recipient mice modulated the extent that DC competitively repopulated the spleen (e.g., wt/HVEM \rightarrow wt vs \rightarrow HVEM). Thus, HVEM and BTLA signals provided by the splenic stromal micro-environment also influence inhibitory signaling that maintains DC homeostasis. Furthermore, wt DC were also impacted in the mixed chimeras reflected by the increased CD8 α - DC subsets (ratio = 0.3) independently of recipient background. This effect of HVEM or BTLA deficiency on wt cells is consistent with cellular interactions in trans with neighboring DC that provide inhibitory signaling regulating proliferation and accumulation. Thus, DC interactions with other DC and with the stromal microenvironment provide sources of inhibitory signaling, although the directional flow of signals between these various cell types requires further elucidation.

Evidence that the CD8 α + DC population is subject to regulation by HVEM was found in the competitive repopulation chimera experiment (specific increase in CD8 α DC subset $r = 0.6$) and in the LT β /LIGHT/HVEM triple deficient mice (Fig. 5B). HVEM deletion by itself had no effect on CD8 α DC subset, however in the triple deficient mouse, a specific decrease in the CD8 α DC subset occurred relative to LT β /LIGHT^{-/-} mice, along with an increase in CD4⁺ DC subset, resetting the CD8 α /CD4 subset ratio. The basis of the HVEM phenotype is unclear but is distinct from that observed in BTLA^{-/-} mice. This result could be interpreted as a composite phenotype that includes positive signaling by HVEM promoting CD8 α + subset, and a loss of inhibitory signaling on the CD4⁺ subset via the HVEM-BTLA pathway, together restoring a normal ratio of CD8 α /CD4⁺ subsets.

The genetic evidence indicates LT α β -LT β R-NIK-RelB pathway provides positive signals for DC proliferation. The HVEM-BTLA checkpoint in wt and LT β /LIGHT deficient mice was bypassed with sustained LT β R signaling (agonist anti-LT β R antibody), suggesting the LT β R pathway acts dominantly to HVEM-BTLA (Fig. 7). Additionally, the finding that there was no change in the percentage of BrdU-labeled DC in either HVEM^{-/-} or BTLA^{-/-} mice when compared with wt mice suggests that the inhibitory effect of HVEM-BTLA pathway does not directly impinge on the LT β R driven proliferation. This interpretation seems appropriate in view of the signaling mechanism known for BTLA. The ITIM motif in BTLA is thought to mediate inhibitory signaling through recruitment of SHP1 tyrosine phosphatase, which does not act on substrates targeted by serine kinases NIK or IKK α involved in LT β R activation of RelB. These results indicate LT β R signaling pathway is not directly altered, and in view of BrdU labeling experiment, suggest that HVEM-BTLA pathway may impact a post mitotic phase of DC differentiation, the target of which is unknown.

Different DC subsets appear to influence the quality of T cell responses. CD8 α + DC appear to favor the development proinflammatory TH1 responses because of their potential to produce of high levels of IL-12, whereas CD8 α - DC subsets are more potent at inducing TH2 responses (5). However, DC subset directed T cell responses may vary depending on type of costimulation and Ag (53). The CD8 α + DC subpopulation has the capacity to capture apoptotic cell-associated Ags activating CD8⁺ T cells by cross-priming (54,55). Thus, the reduction of CD8 α - DC subsets may explain in part the alteration of some T cell responses described in LT-

deficient mice (56,57) and enhanced responses in BTLA deficient mice (58,59). T cell expression of LT α impacts the maturation of DC (60). Alteration of LT β R and HVEM-BTLA signaling potential by pharmacological intervention may impact DC subsets required for de novo and persistent Ag presentation, and thus impact the quality of cellular immune responses.

Acknowledgments

We thank Ian Humphreys and Pedro Ruiz for helpful discussions, and Ginelle Patterson, Lisa Hohmann, and Heather Mar for technical assistance.

References

- Banchereau J, Briere F, Caux C, Davoust J, Lebecque S, Liu YJ, Pulendran B, Palucka K. Immunobiology of dendritic cells. *Annu. Rev. Immunol* 2000;18:767–811. [PubMed: 10837075]
- Vremec D, Pooley J, Hochrein H, Wu L, Shortman K. CD4 and CD8 expression by dendritic cell subtypes in mouse thymus and spleen. *J. Immunol* 2000;164:2978–2986. [PubMed: 10706685]
- Leenen PJ, Radosevich K, Voerman JS, Salomon B, van Rooijen N, Klatzmann D, van Ewijk W. Heterogeneity of mouse spleen dendritic cells: in vivo phagocytic activity, expression of macrophage markers, and subpopulation turnover. *J. Immunol* 1998;160:2166–2173. [PubMed: 9498754]
- Maldonado-Lopez R, De Smedt T, Michel P, Godfroid J, Pajak B, Heirman C, Thielemans K, Leo O, Urbain J, Moser M. CD8 α^+ and CD8 α^- subclasses of dendritic cells direct the development of distinct T helper cells in vivo. *J. Exp. Med* 1999;189:587–592. [PubMed: 9927520]
- Maldonado-Lopez R, Moser M. Dendritic cell subsets and the regulation of Th1/Th2 responses. *Semin. Immunol* 2001;13:275–282. [PubMed: 11502162]
- Asselin-Paturel C, Boonstra A, Dalod M, Durand I, Yessaad N, Dezutter-Dambuyant C, Vicari A, O'Garra A, Biron C, Briere F, Trinchieri G. Mouse type I IFN-producing cells are immature APCs with plasmacytoid morphology. *Nat. Immunol* 2001;2:1144–1150. [PubMed: 11713464]
- Martin P, Del Hoyo GM, Anjuere F, Arias CF, Vargas HH, Fernandez LA, Parrillas V, Ardavin C. Characterization of a new subpopulation of mouse CD8 α^+ B220 $^+$ dendritic cells endowed with type 1 interferon production capacity and tolerogenic potential. *Blood* 2002;100:383–390. [PubMed: 12091326]
- Henri S, Vremec D, Kamath A, Waithman J, Williams S, Benoist C, Burnham K, Saeland S, Handman E, Shortman K. The dendritic cell populations of mouse lymph nodes. *J. Immunol* 2001;167:741–748. [PubMed: 11441078]
- Ardavin C. Origin, precursors and differentiation of mouse dendritic cells. *Nat. Rev. Immunol* 2003;3:582–590. [PubMed: 12876560]
- Ardavin C, Wu L, Li CL, Shortman K. Thymic dendritic cells and T cells develop simultaneously in the thymus from a common precursor population. *Nature* 1993;362:761–763. [PubMed: 8469288]
- Wu L, Li CL, Shortman K. Thymic dendritic cell precursors: relationship to the T lymphocyte lineage and phenotype of the dendritic cell progeny. *J. Exp. Med* 1996;184:903–911. [PubMed: 9064350]
- Traver D, Akashi K, Manz M, Merad M, Miyamoto T, Engleman EG, Weissman IL. Development of CD8 α -positive dendritic cells from a common myeloid progenitor. *Science* 2000;290:2152–2154. [PubMed: 11118150]
- Manz MG, Traver D, Miyamoto T, Weissman IL, Akashi K. Dendritic cell potentials of early lymphoid and myeloid progenitors. *Blood* 2001;97:3333–3341. [PubMed: 11369621]
- Wu L, D'Amico A, Hochrein H, O'Keeffe M, Shortman K, Lucas K. Development of thymic and splenic dendritic cell populations from different hemopoietic precursors. *Blood* 2001;98:3376–3382. [PubMed: 11719377]
- Naik SH, Metcalf D, van Nieuwenhuijze A, Wicks I, Wu L, O'Keeffe M, Shortman K. Intrasplenic steady-state dendritic cell precursors that are distinct from monocytes. *Nat. Immunol* 2006;7:663–671. [PubMed: 16680143]
- Aliberti J, Schulz O, Pennington DJ, Tsujimura H, Reis e Sousa C, Ozato K, Sher A. Essential role for ICSBP in the in vivo development of murine CD8 α^+ dendritic cells. *Blood* 2003;101:305–310. [PubMed: 12393690]

17. Hacker C, Kirsch RD, Ju XS, Hieronymus T, Gust TC, Kuhl C, Jorgas T, Kurz SM, Rose-John S, Yokota Y, Zenke M. Transcriptional profiling identifies Id2 function in dendritic cell development. *Nat. Immunol* 2003;4:380–386. [PubMed: 12598895]
18. Yamaoka K, Min B, Zhou YJ, Paul WE, O'Shea J. Jak3 negatively regulates dendritic cell cytokine production and survival. *Blood* 2005;106:3227–3233. [PubMed: 16020505]
19. Wu L, Nichogiannopoulou A, Shortman K, Georgopoulos K. Cell-autonomous defects in dendritic cell populations of Ikaros mutant mice point to a developmental relationship with the lymphoid lineage. *Immunity* 1997;7:483–492. [PubMed: 9354469]
20. Guerriero A, Langmuir PB, Spain LM, Scott EW. PU.1 is required for myeloid-derived but not lymphoid-derived dendritic cells. *Blood* 2000;95:879–885. [PubMed: 10648399]
21. Ichikawa E, Hida S, Omatsu Y, Shimoyama S, Takahara K, Miyagawa S, Inaba K, Taki S. Defective development of splenic and epidermal CD4⁺ dendritic cells in mice deficient for IFN regulatory factor-2. *Proc. Natl. Acad. Sci. USA* 2004;101:3909–3914. [PubMed: 15004277]
22. Caton ML, Smith-Raska MR, Reizis B. Notch-RBP-J signaling controls the homeostasis of CD8⁻ dendritic cells in the spleen. *J. Exp. Med* 2007;204:1653–1664. [PubMed: 17591855]
23. Suzuki S, Honma K, Matsuyama T, Suzuki K, Toriyama K, Akitoyo I, Yamamoto K, Suematsu T, Nakamura M, Yui K, Kumatori A. Critical roles of interferon regulatory factor 4 in CD11b^{high} CD8^{α-} dendritic cell development. *Proc. Natl. Acad. Sci. USA* 2004;101:8981–8986. [PubMed: 15184678]
24. Kobayashi T, Walsh PT, Walsh MC, Speirs KM, Chiffolleau E, King CG, Hancock WW, Caamano JH, Hunter CA, Scott P, Turka LA, Choi Y. TRAF6 is a critical factor for dendritic cell maturation and development. *Immunity* 2003;19:353–363. [PubMed: 14499111]
25. Wu L, D'Amico A, Winkel KD, Suter M, Lo D, Shortman K. RelB is essential for the development of myeloid-related CD8^{α-} dendritic cells but not of lymphoid-related CD8^{α+} dendritic cells. *Immunity* 1998;9:839–847. [PubMed: 9881974]
26. Kabashima K, Banks TA, Ansel KM, Lu TT, Ware CF, Cyster JG. Intrinsic lymphotoxin-β receptor requirement for homeostasis of lymphoid tissue dendritic cells. *Immunity* 2005;22:439–450. [PubMed: 15845449]
27. Abe K, Yarovsky FO, Murakami T, Shakhov AN, Tumanov AV, Ito D, Drutskaya LN, Pfeffer K, Kuprash DV, Komschlies KL, Nedospasov SA. Distinct contributions of TNF and LT cytokines to the development of dendritic cells in vitro and their recruitment in vivo. *Blood* 2003;101:1477–1483. [PubMed: 12560241]
28. DeJardin E, Droin NM, Delhase M, Haas E, Cao Y, Makris C, Li ZW, Karin M, Ware CF, Green DR. The lymphotoxin-β receptor induces different patterns of gene expression via two NF-κB pathways. *Immunity* 2002;17:525–535. [PubMed: 12387745]
29. Mauri ND, Ebner R, Montgomery RI, Kochel KD, Cheung TC, Yu G-L, Ruben S, Murphy M, Eisenbery RJ, Cohen GH, et al. LIGHT: a new member of the TNF superfamily and lymphotoxin α are ligands for herpes-virus entry mediator. *Immunity* 1998;8:21–30. [PubMed: 9462508]
30. Ware CF. Network communications: lymphotoxins, LIGHT, and TNF. *Annu. Rev. Immunol* 2005;23:787–819. [PubMed: 15771586]
31. Watts TH. TNF/TNFR family members in costimulation of T cell responses. *Annu. Rev. Immunol* 2005;23:23–68. [PubMed: 15771565]
32. Sedy JR, Gavrieli M, Potter KG, Hurchla MA, Lindsley RC, Hildner K, Scheu S, Pfeffer K, Ware CF, Murphy TL, Murphy KM. B and T lymphocyte attenuator regulates T cell activation through interaction with herpesvirus entry mediator. *Nat. Immunol* 2005;6:90–98. [PubMed: 15568026]
33. Gavrieli M, Murphy KM. Association of Grb-2 and PI3K p85 with phosphotyrosine peptides derived from BTLA. *Biochem. Biophys. Res. Commun* 2006;345:1440–1445. [PubMed: 16725108]
34. Chemnitz JM, Lanfranco AR, Braunstein I, Riley JL. B and T lymphocyte attenuator-mediated signal transduction provides a potent inhibitory signal to primary human CD4 T cells that can be initiated by multiple phosphotyrosine motifs. *J. Immunol* 2006;176:6603–6614. [PubMed: 16709818]
35. Cheung TC, Humphreys IR, Potter KG, Norris PS, Shumway HM, Tran BR, Patterson G, Jean-Jacques R, Yoon M, Spear PG, et al. Evolutionarily divergent herpesviruses modulate T cell activation by targeting the herpesvirus entry mediator cosignaling pathway. *Proc. Natl. Acad. Sci. USA* 2005;102:13218–13223. [PubMed: 16131544]

36. Compaan DM, Gonzalez LC, Tom I, Loyet KM, Eaton D, Hymowitz SG. Attenuating lymphocyte activity: the crystal structure of the BTLA-HVEM complex. *J. Biol. Chem* 2005;280:39553–39561. [PubMed: 16169851]
37. Gonzalez LC, Loyet KM, Calemine-Fenaux J, Chauhan V, Wranik B, Ouyang W, Eaton DL. A coreceptor interaction between the CD28 and TNF receptor family members B and T lymphocyte attenuator and herpesvirus entry mediator. *Proc. Natl. Acad. Sci. USA* 2005;102:1116–1121. [PubMed: 15647361]
38. Murphy KM, Nelson CA, Sedy JR. Balancing co-stimulation and inhibition with BTLA and HVEM. *Nat. Rev. Immunol* 2006;6:671–681. [PubMed: 16932752]
39. Krieg C, Boyman O, Fu YX, Kaye J. B and T lymphocyte attenuator regulates CD8⁺ T cell-intrinsic homeostasis and memory cell generation. *Nat. Immunol* 2007;8:162–171. [PubMed: 17206146]
40. Hurchla MA, Sedy JR, Gavrielli M, Drake CG, Murphy TL, Murphy KM. B and T lymphocyte attenuator exhibits structural and expression polymorphisms and is highly induced in anergic CD4⁺ T cells. *J. Immunol* 2005;174:3377–3385. [PubMed: 15749870]
41. Truong W, Hancock WW, Anderson CC, Merani S, Shapiro AM. Coinhibitory T-cell signaling in islet allograft rejection and tolerance. *Cell Transplant* 2006;15:105–119. [PubMed: 16719045]
42. Futterer A, Mink K, Luz A, Kosco-Vilbois MH, Pfeffer K. The lymphotoxin β receptor controls organogenesis and affinity maturation in peripheral lymphoid tissues. *Immunity* 1998;9:59–70. [PubMed: 9697836]
43. Scheu S, Alferink J, Potzel T, Barchet W, Kalinke U, Pfeffer K. Targeted disruption of LIGHT causes defects in costimulatory T Cell activation and reveals cooperation with lymphotoxin β in mesenteric lymph node genesis. *J. Exp. Med* 2002;195:1613–1624. [PubMed: 12070288]
44. Alimzhanov MB, Kuprash DV, Kosco-Vilbois MH, Luz A, Turetskaya RL, Tarakhovsky A, Rajewsky K, Nedospasov SA, Pfeffer K. Abnormal development of secondary lymphoid tissues in lymphotoxin β -deficient mice. *Proc. Natl. Acad. Sci. USA* 1997;94:9302–9307. [PubMed: 9256477]
45. Wang Y, Subudhi SK, Anders RA, Lo J, Sun Y, Blink S, Wang Y, Wang J, Liu X, Mink K, et al. The role of herpesvirus entry mediator as a negative regulator of T cell-mediated responses. *J. Clin. Invest* 2005;115:711–717. [PubMed: 15696194]
46. Shinkura R, Kitada K, Matsuda F, Tashiro K, Ikuta K, Suzuki M, Kogishi K, Serikawa T, Honjo T. A lymphoplasia is caused by a point mutation in the mouse gene encoding NF- κ B-inducing kinase. *Nat. Genet* 1999;22:74–77. [PubMed: 10319865]
47. Watanabe N, Gavrielli M, Sedy JR, Yang J, Fallarino F, Loftin SK, Hurchla MA, Zimmerman N, Sim J, Zang X, et al. BTLA is a lymphocyte inhibitory receptor with similarities to CTLA-4 and PD-1. *Nat. Immunol* 2003;4:670–679. [PubMed: 12796776]
48. Banks TA, Rickert S, Benedict CA, Ma L, Ko M, Meier J, Ha W, Schneider K, Granger SW, Turovskaya O, et al. A lymphotoxin-IFN- β axis essential for lymphocyte survival revealed during cytomegalovirus infection. *J. Immunol* 2005;174:7217–7225. [PubMed: 15905567]
49. Liu K, Waskow C, Liu X, Yao K, Hoh J, Nussenzweig M. Origin of dendritic cells in peripheral lymphoid organs of mice. *Nat. Immunol* 2007;8:578–583. [PubMed: 17450143]
50. Hauer J, Puschner S, Ramakrishnan P, Simon U, Bongers M, Federle C, Engelmann H. TNF receptor (TNFR)-associated factor (TRAF) 3 serves as an inhibitor of TRAF2/5-mediated activation of the noncanonical NF- κ B pathway by TRAF-binding TNFRs. *Proc. Natl. Acad. Sci. USA* 2005;102:2874–2879. [PubMed: 15708970]
51. Rennert PD, James D, Mackay F, Browning JL, Hochman PS. Lymph node genesis is induced by signaling through the lymphotoxin β receptor. *Immunity* 1998;9:71–80. [PubMed: 9697837]
52. Drayton DL, Bonizzi G, Ying X, Liao S, Karin M, Ruddle NH. I κ B kinase complex α kinase activity controls chemokine and high endothelial venule gene expression in lymph nodes and nasal-associated lymphoid tissue. *J. Immunol* 2004;173:6161–6168. [PubMed: 15528353]
53. Skokos D, Nussenzweig MC. CD8- DCs induce IL-12-independent Th1 differentiation through δ 4 notch-like ligand in response to bacterial LPS. *J. Exp. Med* 2007;204:1525–1531. [PubMed: 17576775]
54. den Haan JM, Lehar SM, Bevan MJ. CD8⁺ but not CD8⁻ dendritic cells cross-prime cytotoxic T cells in vivo. *J. Exp. Med* 2000;192:1685–1696. [PubMed: 11120766]

55. Schulz O, Reis e Sousa C. Cross-presentation of cell-associated antigens by CD8 α ⁺ dendritic cells is attributable to their ability to internalize dead cells. *Immunology* 2002;107:183–189. [PubMed: 12383197]
56. Kumaraguru U, Davis IA, Deshpande S, Tevethia SS, Rouse BT. Lymphotoxin α [minus/minus] mice develop functionally impaired CD8⁺ T cell responses and fail to contain virus infection of the central nervous system. *J. Immunol* 2001;166:1066–1074. [PubMed: 11145686]
57. Lund FE, Partida-Sanchez S, Lee BO, Kusser KL, Hartson L, Hogan RJ, Woodland DL, Randall TD. Lymphotoxin- α -deficient mice make delayed, but effective, T and B cell responses to influenza. *J. Immunol* 2002;169:5236–5243. [PubMed: 12391242]
58. Han P, Goularte OD, Rufner K, Wilkinson B, Kaye J. An inhibitory Ig superfamily protein expressed by lymphocytes and APCs is also an early marker of thymocyte positive selection. *J. Immunol* 2004;172:5931–5939. [PubMed: 15128774]
59. Tao R, Wang L, Han R, Wang T, Ye Q, Honjo T, Murphy TL, Murphy KM, Hancock WW. Differential effects of B and T lymphocyte attenuator and programmed death-1 on acceptance of partially versus fully MHC-mismatched cardiac allografts. *J. Immunol* 2005;175:5774–5782. [PubMed: 16237069]
60. Summers-DeLuca LE, McCarthy DD, Cosovic B, Ward LA, Lo CC, Scheu S, Pfeffer K, Gommerman JL. Expression of lymphotoxin- $\alpha\beta$ on antigen-specific T cells is required for DC function. *J. Exp. Med* 2007;204:1071–1081. [PubMed: 17452522]

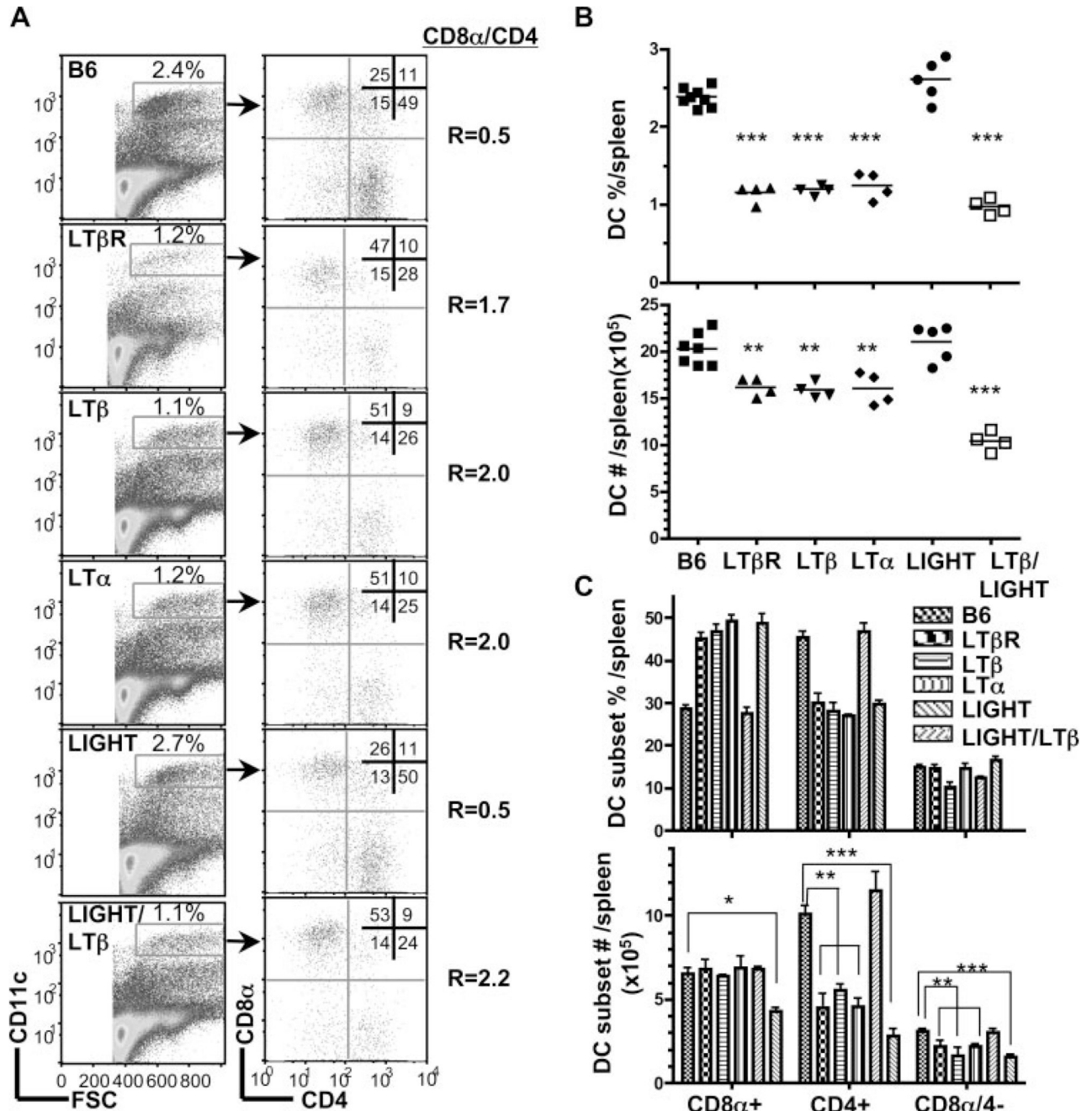


FIGURE 1. LTαβ-LTβR interaction mediates homeostasis of CD8⁻ DC subsets. *A*, CD11c^{high} cells in the spleen were analyzed for CD4 and CD8α expression in wt B6, LTβR⁻, LTβ⁻, LTα⁻, LIGHT⁻ and LTβ/LIGHT-deficient mice by flow cytometry as described in *Materials and Methods*. A representative histogram is shown for each mouse strain. The ratio of CD8α to CD4 DC subsets was calculated from values in the upper left and lower right quadrants. *B*, The percentage of DC are presented as a fraction of total nucleated splenocytes (*top panel*) and the total number of DC (*bottom panel*) in the spleen from the indicated gene deficient mice. Each data point represents an individual animal and the data are pooled from two analyses. *C*, The percentage (*top panel*) and total number (*bottom panel*) of individual CD4⁺, CD8α⁺, and CD8α⁻/CD4⁻ DC

subsets within the gated CD11c^{high} DC. The bars are the mean \pm SD from at least three mice per group and the data are representative of three independent experiments. In all panels, Student *t* test evaluation of significance where *, **, and *** denote $p < 0.05$, $p < 0.01$, and $p < 0.001$, respectively, between the indicated groups.

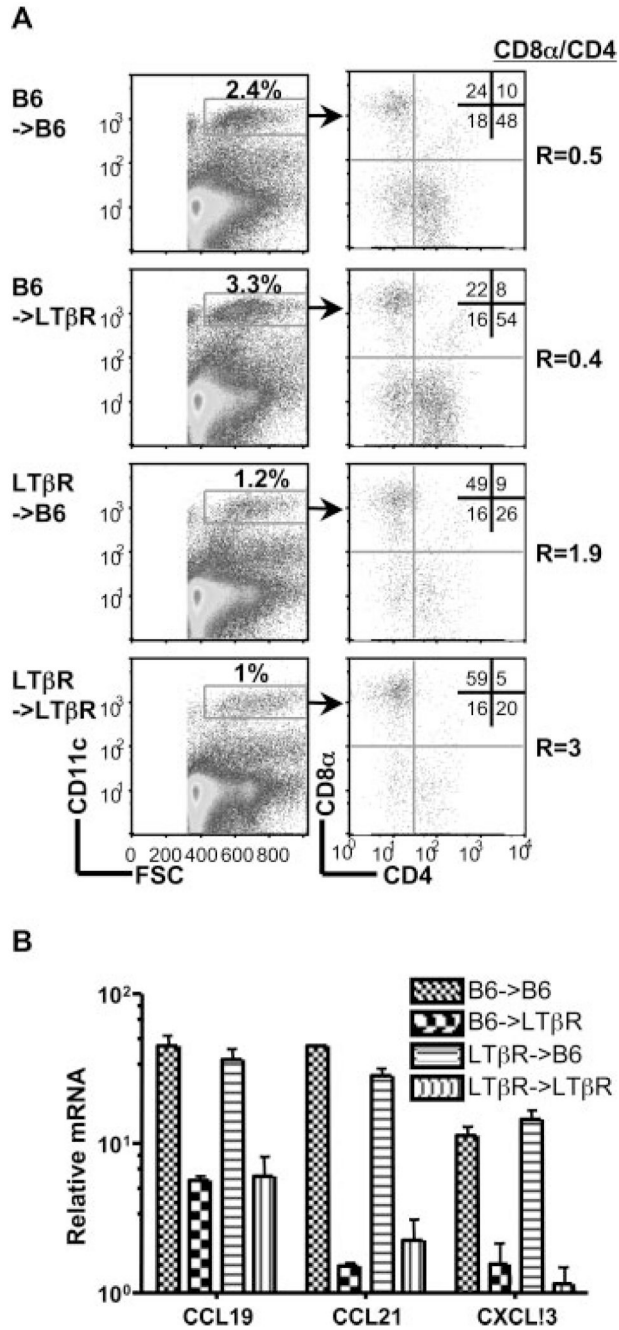


FIGURE 2. Homeostasis of splenic DC subsets is independent of the lymphoid tissue organizing chemokines. *A*, Eight weeks after bone marrow reconstitution, splenocytes within the CD11c^{high} population (gates indicated in figure) were analyzed for expression of CD4 and CD8α. A representative histogram is shown for each group of chimeras and is representative of two independent experiments. The ratio of CD8α to CD4 DC subsets was calculated from values in the upper left and lower right quadrants. *B*, Quantitative PCR analysis of chemokine mRNA expressed in the spleen from the bone marrow chimeras is presented as the relative amount of indicated mRNA normalized to 18S. Error bars are the mean±SD from at least two mice per group and the data are representative of two independent experiments.

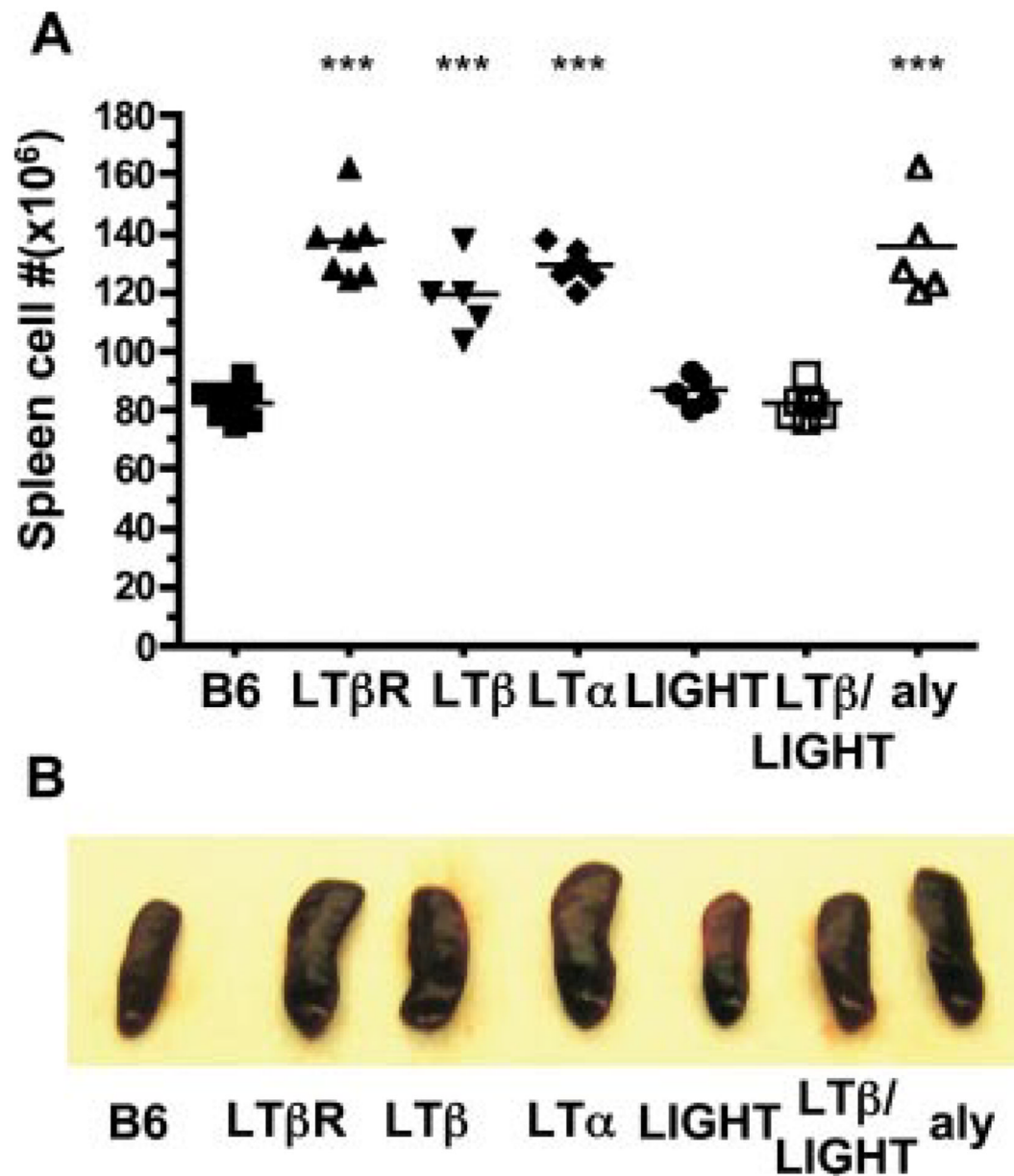


FIGURE 3.

Counter regulatory effects of LIGHT and LT $\alpha\beta$ -LT β R on splenic size and cellularity. *A*, The total number of spleen cells were determined in wt B6, LT β R, LT β -, LT α -, LIGHT-, LT β /LIGHT-deficient and *aly* mice. Each point represents the value obtained from an individual animal and the data are from five pooled experiments. *B*, Representative spleens from mice deficient in LT β R, LT β , LT α , LIGHT, and LT β /LIGHT, or mutant *aly* and wt B6 mice. Student *t* test significance between the wt B6 and the other groups $p < 0.001$ (*).

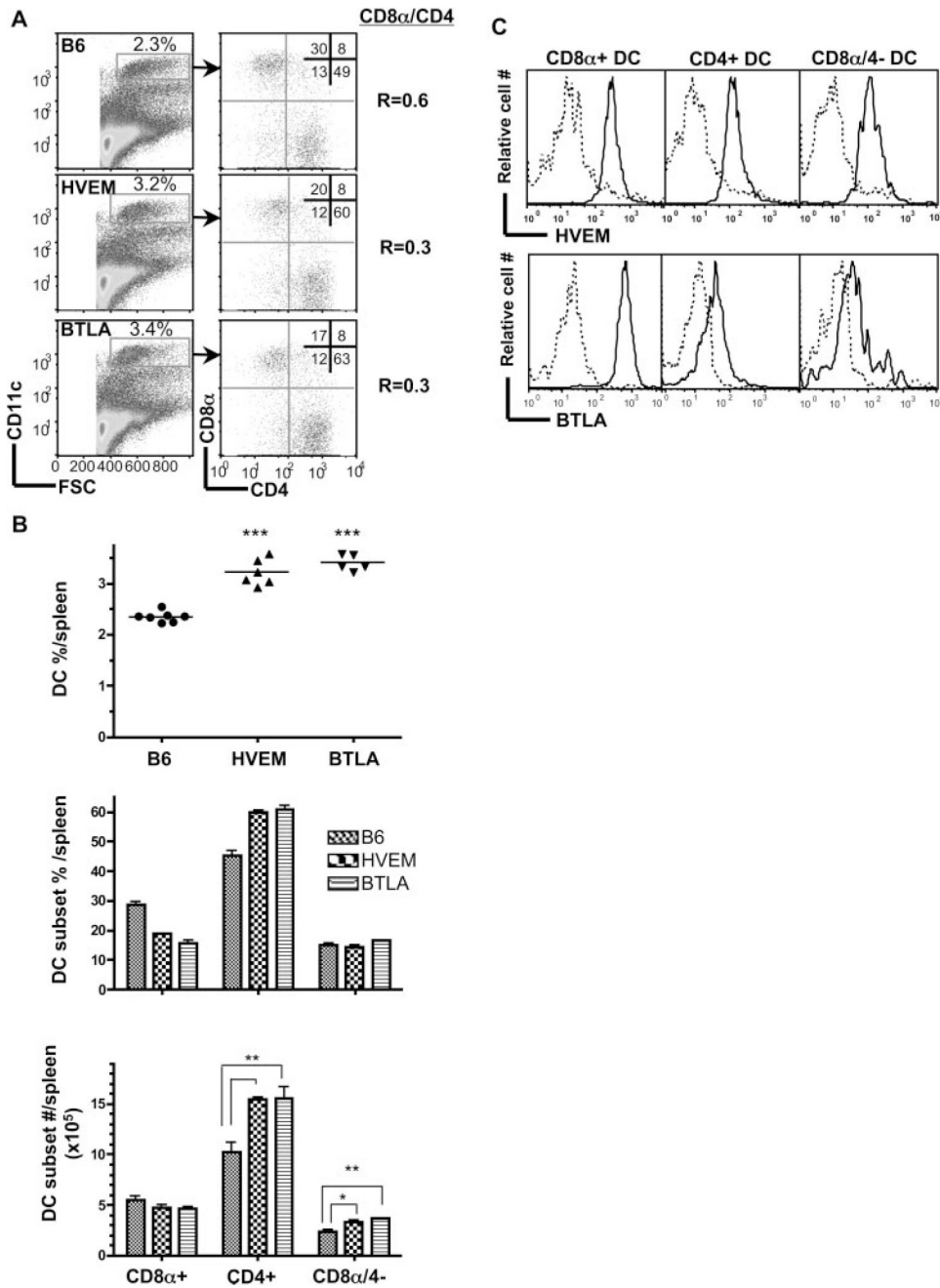
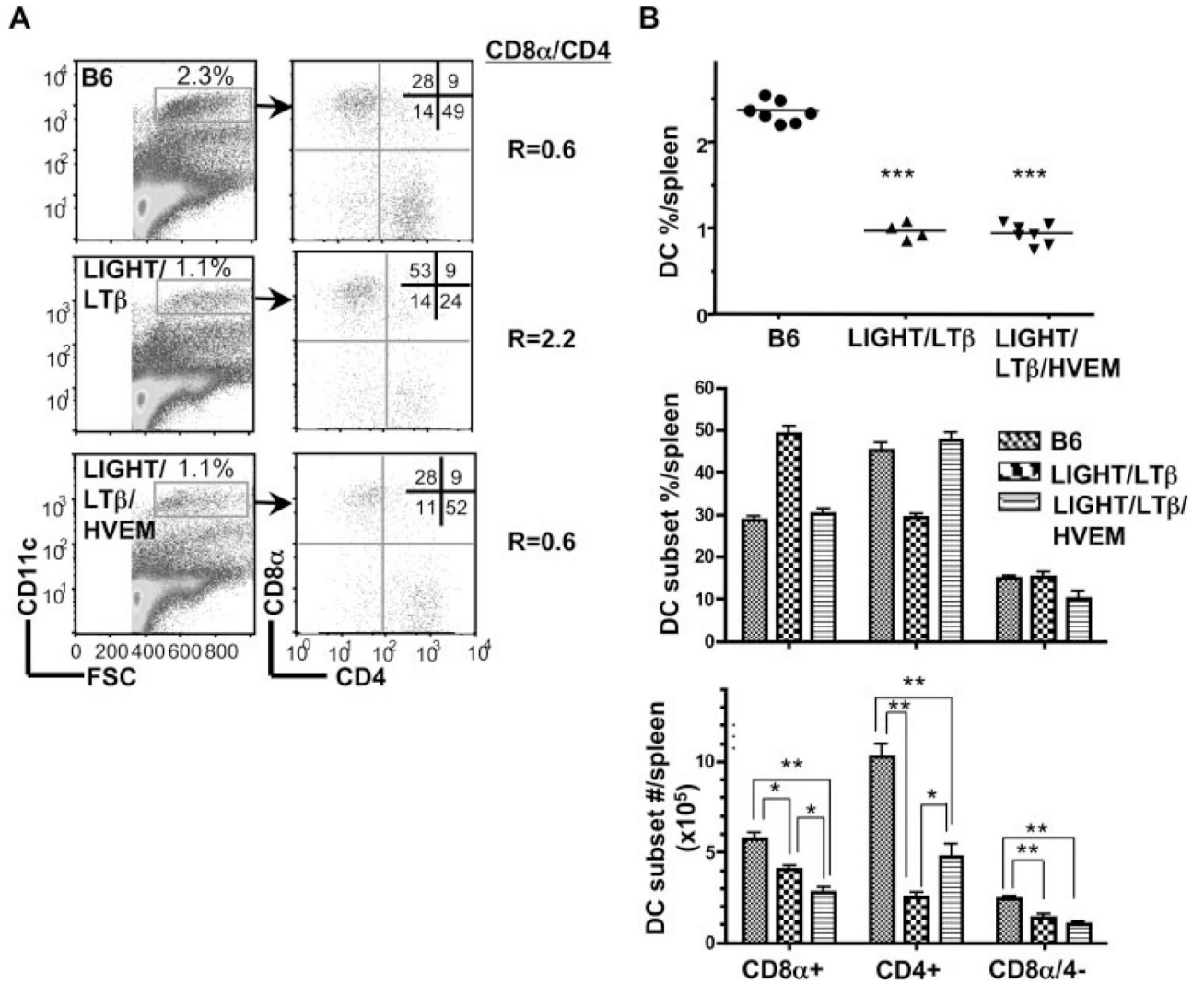
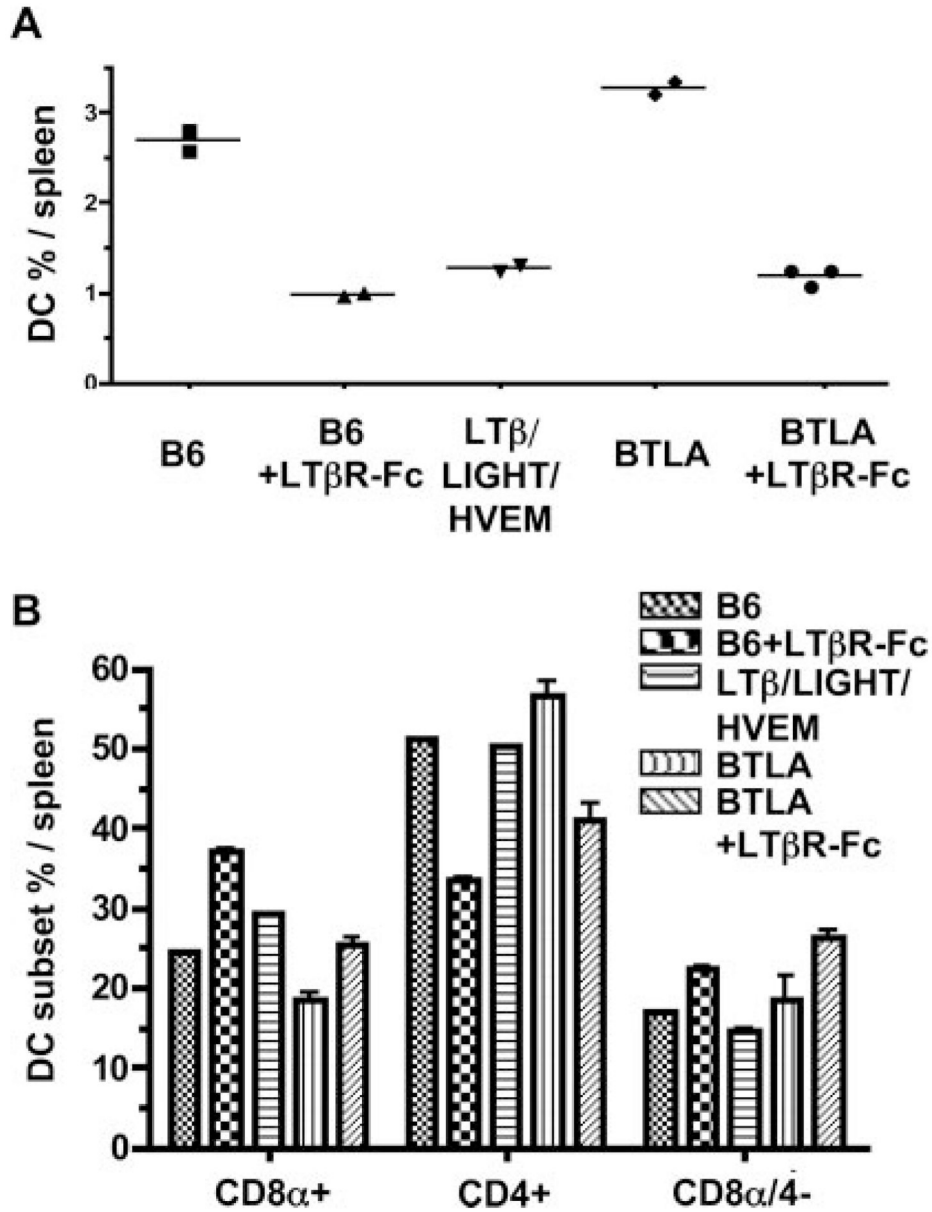


FIGURE 4. HVEM and BTLA counter regulate homeostasis of CD4⁺ and CD4⁻ CD8α⁻ DC subsets. *A*, CD11c^{high} cells gated as indicated were analyzed for CD4 and CD8α expression in wt B6, HVEM- or BTLA-deficient mice. A representative histogram is shown for each mouse strain. The ratio of CD8α to CD4 DC subsets was calculated from values in the upper left and lower right quadrants. *B*, The percentage of DC as a fraction of total nucleated splenocytes (*top panel*), the percentage of individual DC subsets (*middle panel*) and the total number cells in each DC subset (*bottom panel*) in the spleen from the indicated gene-deficient mice. Each data point represents the value obtained from an individual animal and the data are pooled from two analyses. Bars show the mean ± SD from at least *n* = three mice per group and the data are

representative of three independent experiments. Student's *t* test was performed where *, **, and *** denote significance of $p < 0.05$, $p < 0.01$, and $p < 0.001$, respectively, between the indicated groups. C, Flow cytometric analysis of HVEM and BTLA expression by CD8 α^+ , and CD4 $^+$ CD8 $^-$ DC subsets within gated DC from WT (solid line) and HVEM-deficient mice (dashed line) and WT mice (BTLA staining = solid line and ctrl staining = dashed line), respectively.

**FIGURE 5.**

LIGHT/LTβ/HVEM mice reveal an LT-independent DC subset with normal CD8α/CD4 subset ratio. A. CD11c^{high} cells gated as indicated were analyzed for CD4 and CD8α expression in WT B6, LTβ/LIGHT, and LTβ/LIGHT/HVEM-deficient mice as described in the *Materials and Methods*. A representative histogram is shown for each mouse strain. The ratio of CD8α to CD4 DC subsets was calculated from values in the upper left and lower right quadrants. B. The percentage of DC as a fraction of total nucleated splenocytes (*top panel*), the percentage of individual DC subsets (*middle panel*) and the total number cells in each DC subset (*bottom panel*) in the spleen from the indicated gene deficient mice were calculated from flow data. Each data point represents the value obtained from an individual animal and the data are pooled from two analyses. Bars show the mean ± SD from at least three mice per group, and the data are representative of three independent experiments. Student's *t* test was performed where *, **, and *** denote significance of $p < 0.05$, $p < 0.01$, and $p < 0.001$, respectively, between the indicated groups.

**FIGURE 6.**

DC subsets in $LT\beta R$ -Fc-treated $BTLA^{-/-}$ mice. **A**, The percentage of DC in $LIGHT/LT\beta/HVEM$ - and $BTLA$ -deficient as well as wt B6 and $LT\beta R$ -Fc-treated B6 mice are presented as the percentage of total nucleated splenocytes. Mice were treated with the mouse $LT\beta R$ -Fc fusion protein as described in the methods. **B**, The percentage of individual $CD4^+$, $CD8\alpha$, and $CD8\alpha/CD4^-$ DC subsets within the gated $CD11c^{high}$ DC. Each data point represents the value obtained from an individual animal. Bars show the mean \pm SD from at least $n = 2$ mice per group and the data are representative of two independent experiments.

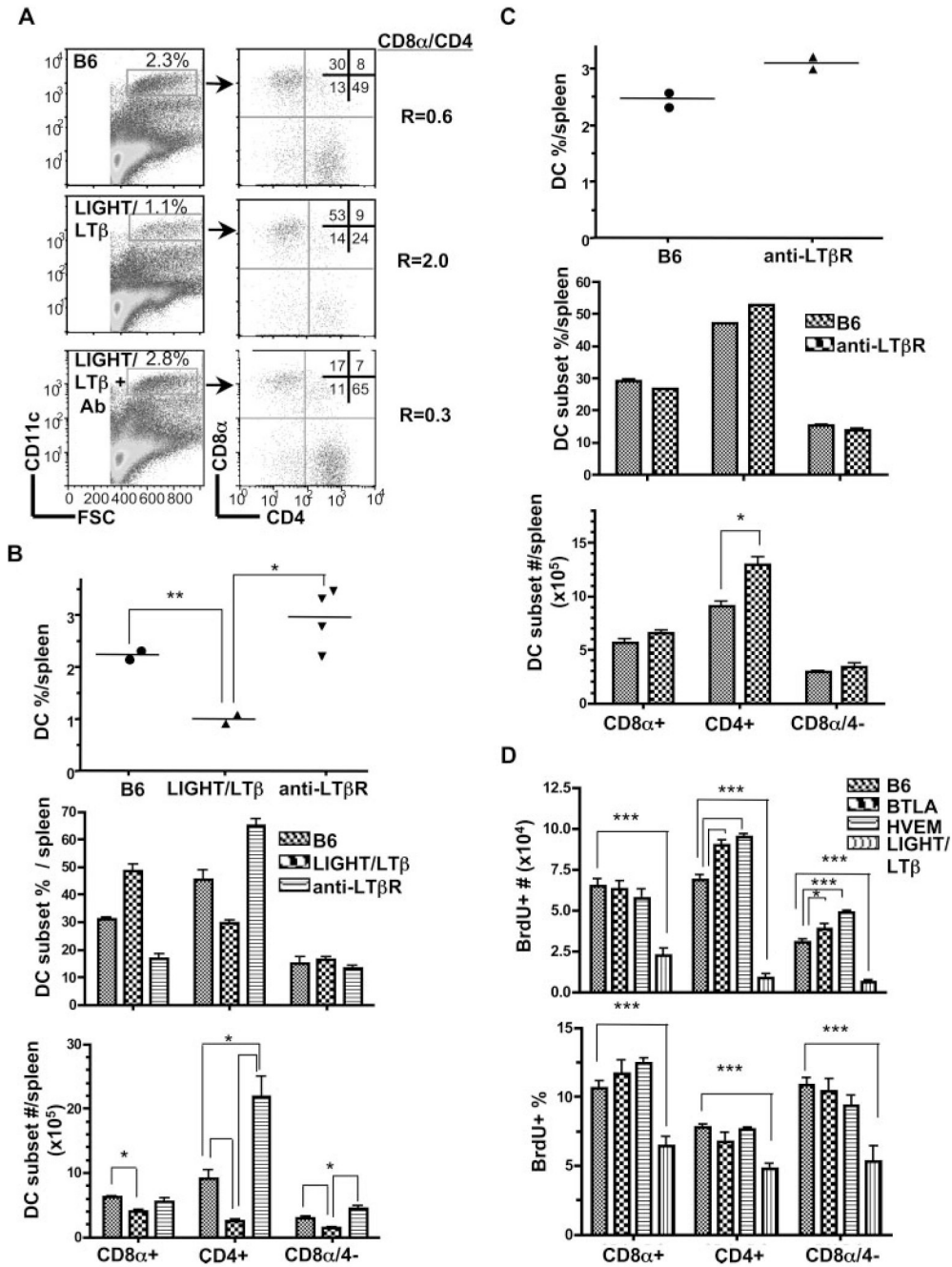


FIGURE 7. Activation of LTβR signaling restores DC homeostasis. *A*, CD11c^{high} cells gated as indicated were analyzed for CD4 and CD8α expression in wt B6, LIGHT/LTβ-deficient mice (untreated), and LTβ/LIGHT treated with rat anti-mouse LTβR mAb as described in the *Materials and Methods*. A representative histogram is shown for each mouse strain. The ratio of CD8α to CD4 DC subsets was calculated from values in the upper left and lower right quadrants. *B*, The percentage of DC as a fraction of total nucleated splenocytes (*top panel*), the percentage of individual DC subsets (*middle panel*) and the total number cells in each DC subset (*bottom panel*) in the spleen from the indicated gene-deficient or mAb-treated mice. Each data point represents the value obtained from an individual animal. Bars show the mean ± SD from at

least $n =$ three mice per group and the data are representative of three independent experiments. Student's test was performed where * and ** denote a significance of $p < 0.05$ and $p < 0.01$, respectively, between the indicated groups. *C*, The effect of LT β R activation in wt B6 mice on DC subsets. The percentage of DC as a fraction of total nucleated splenocytes (*top panel*), the percentage of individual DC subsets (*middle panel*) and the total number cells in each DC subset (*bottom panel*) in the spleen from wt B6 or rat anti-mouse LT β R treated mice (as in *A*). Bars show the mean \pm SD from at least two mice per group and the data are representative of two independent experiments. Student *t* test significance between the wt B6 and the other groups $p < 0.05$ (*). *D*, Total number (*top panel*) and frequency (*bottom panel*) of BrdU⁺ cells CD8 α ⁺, CD4⁺, and CD8 α /CD4⁻ DC in the spleen of wt B6, HVEM⁻, BTLA⁻ and LIGHT/LT β -deficient mice treated with BrdU for 16 h. Bars show the mean \pm SD from at least three mice per group and the data are representative of two independent experiments. Student's test was performed where * and *** denote significance of $p < 0.05$ and $p < 0.001$, respectively, between the indicated groups.

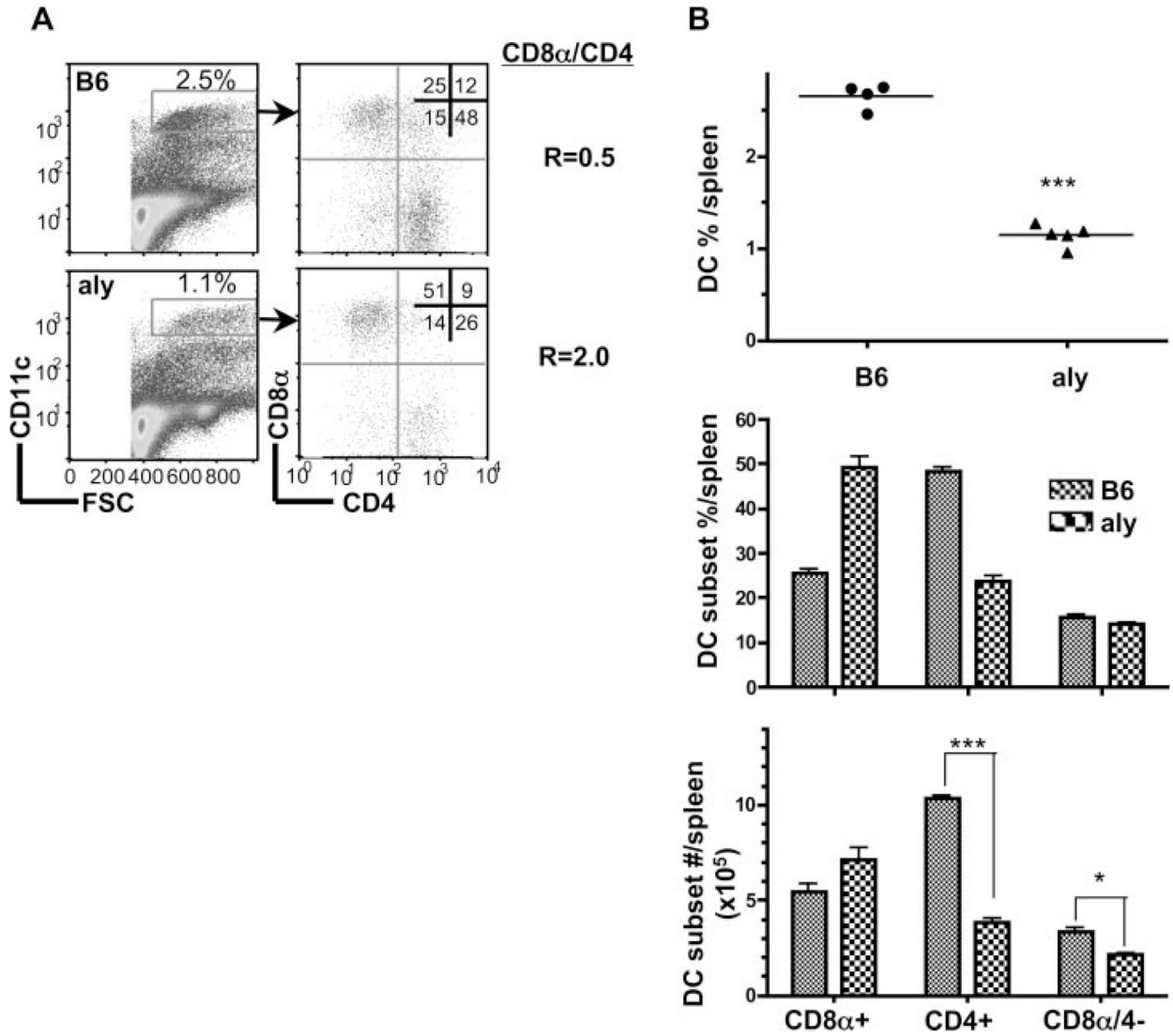


FIGURE 8. Alymphoplasia (NIK mutant) mice have a specific defect in CD8α⁻ DC subsets. *A*, CD11c^{high} cells were analyzed for CD4 and CD8α expression from wt B6 and *aly* mice as described in the *Materials and Methods*. *B*, The percentage of DC as a fraction of total nucleated splenocytes (*top panel*), the percentage of individual DC subsets (*middle panel*) and the total number cells in each DC subset (*bottom panel*) in the spleen from wt B6 and *aly* mice. Each data point represents an individual animal, and the data are pooled from two analyses. Bars show the mean ± SD from at least *n* = three mice per group and the data are representative of three independent experiments. Student’s test was performed where one and three asterisks denote significance of *p* < 0.05 and *p* < 0.001, respectively, between the indicated groups.

Table 1

DC reconstitution in mixed bone marrow chimeras

Live cells and CD11c ^{hi} DC subpopulation		CD45.2/CD45.1 ratio ^d					
Chimera → recipient ^b	Total cells	DC-BTLA ^c		DC-HVEM ^f		DC-CD45.1/4 ^e	
BTLA/wt → wt	1.3	6.2					
BTLA/wt → BTLA	1.0	2.0					
HVEM/wt → wt	1.2			2.8		4.6	
HVEM/wt → HVEM	1.0						

DC Subsets		CD45.1 (%) ^d							
		CD45.2 (%) ^d	CD8α ⁺	CD8α ⁻ 4 ⁻	Ratio CD8α/4 ^e	CD8α ⁺	CD4 ⁺	CD8α ⁻	Ratio CD8α/4 ^e
wt/BTLA → wt	19 ± 6	62 ± 7	14 ± 2	18 ± 2	0.3	16 ± 6	65 ± 11	19 ± 4	0.2
wt/BTLA → BTLA	22 ± 3	53 ± 5	18 ± 2	14 ± 0.2	0.4	22 ± 1	56 ± 3	20 ± 4	0.4
wt/HVEM → wt	29 ± 2	46 ± 4	14 ± 0.2	13 ± 1	0.6	19 ± 5	56 ± 3	25 ± 1	0.3
wt/HVEM → HVEM	29 ± 3	48 ± 3	13 ± 1	13 ± 1	0.6	19 ± 2	58 ± 3	21 ± 0.3	0.3

^aThe two populations of cells expressing allelic forms of CD45 were identified by flow cytometry using the anti-CD45.2 mAb (clone 104). The CD45.2/CD45.1 ratio within the live cell gate was calculated as the sum of the percentage of CD45.2⁺ cells divided by the sum of percentage of CD45.2⁻ cells.

^bMixed bone marrow chimera were made by transferring a 1:1 ratio of CD45.1⁺ C57BL/6 bone marrow cells and CD45.2⁺ HVEM- or BTLA-deficient bone marrow cells into lethally irradiated (10 Gy, Cesium) CD45.1⁺ C57BL/6 (*n* = 2) or CD45.2⁺ HVEM- or BTLA-deficient mice (HVEM; BTLA) (*n* = 3). Spleens from mice were analyzed by flow cytometry 8 wk later.

^cCD45.2/CD45.1 DC ratio was calculated by determining DC with in the FSC-CD11c^{hi} live gate and dividing the sum of the percentage of CD45.2⁺ DC by the sum of the percentage of CD45.2⁻ DC.

^dMean percentage of each DC subset ± SEM for the CD45.2⁺ and CD45.2⁻ populations.

^eThe CD8α/4 DC subset ratio was the calculated sum of the percentage of CD8α DC divided by the sum of the percentage of CD4 DC.